

Low-energy acoustic plasmons at metal surfaces

Bogdan Diaconescu¹, Karsten Pohl¹, Luca Vattuone², Letizia Savio², Philip Hofmann³, Vyacheslav M. Silkin⁴, Jose M. Pitarke⁵, Eugene V. Chulkov⁴, Pedro M. Echenique⁴, Daniel Farías⁶, Mario Rocca⁷

¹*Department of Physics and Material Science Program, University of New Hampshire, Durham NH 03824, USA*

²*CNISM and Dipartimento di Fisica, Università di Genova 16146 Genova, Italy*

³*Institute for Storage Ring Facilities and Interdisciplinary Nanoscience Center (iNANO), University of Aarhus, 8000 Aarhus C, Denmark*

⁴*Donostia International Physics Center (DIPC), Depto. de Física de Materiales and Centro Mixto CSIC-UPV/EHU, Facultad de Ciencias Químicas, UPV/EHU, 20018 San Sebastian, Spain*

⁵*CIC nanoGUNE Consolider and Materia Kondentsatuaren Fisika Saila, UPV/EHU, Mikeletegi Pasealekua 56, E-2009 Donostia, Basque Country, Spain*

⁶*Departamento de Física de la Materia Condensada, Universidad Autónoma de Madrid, 28049 Madrid, Spain*

⁷*IMEM-CNR and Dipartimento di Fisica, Università di Genova 16146 Genova, Italy*

Nearly two-dimensional metallic systems formed in charge inversion layers¹ and artificial layered materials^{2,3} permit the existence of low-energy collective excitations^{4,5}, so-called 2D plasmons, which are not found in a three-dimensional metal. These excitations have caused considerable interest because their low energy allows them to participate in many dynamical

processes involving electrons and phonons³ and as possible candidates to mediate the attractive interaction responsible for the formation of Cooper pairs in high T_c superconductors⁶. Metals often support electronic states that are confined to the surface forming a nearly 2D electron density layer. However, it was argued that these systems could not support low-energy collective excitations because these would be screened out by the underlying bulk electrons⁷. In fact, metallic surfaces should only support the conventional surface plasmons⁸, modes with energies of a few eV, depending only on the electron density, with important applications in surface-plasmon resonance microscopy^{9,10}, photonics and sub-wavelength optics¹¹⁻¹³, but no relevance to the low-energy dynamics. Here we show that, in contrast to this well-established belief, a low-energy collective excitation mode can be found on bare metal surfaces. The mode has an acoustic (linear) dispersion, different to the $q_{\parallel}^{1/2}$ dispersion of a 2D plasmon, and was observed on Be(0001) using angle-resolved electron energy loss spectroscopy. First-principles calculations show that it is caused by the coexistence of a partially occupied quasi 2D surface-state band with the underlying 3D bulk electron continuum and that the non-local character of the dielectric function prevents it from being screened out by the 3D states. The acoustic plasmon reported here has a very general character and should be present on many metal surfaces. Furthermore, the new mode with its acoustic dispersion can allow confinement of light on small surface areas and in a broad frequency range thus being relevant for nano-optics and photonics applications.

The experiment was performed in an ultra high vacuum apparatus at a base pressure of about 2×10^{-10} mbar equipped with an angle-resolved high resolution electron energy loss (EEL) spec-

trometer¹⁴. In most of the measurements the energy resolution was set to about 16 meV. The single crystal Be sample was cut and mechanically polished along the (0001) plane. It was cleaned through repeated 0.5 to 1 keV Ne⁺ sputtering cycles with the sample at 450 °C followed by annealing periods at 500 °C until the amount of oxygen on the surface was below the sensitivity threshold of Auger electron spectroscopy and a fairly sharp low energy electron diffraction pattern was obtained. At this stage EEL spectra still showed the presence of oxygen on the sample, characterized by losses at 80 and 120 meV. Further cleaning resulted in a reduction of the oxygen loss intensity until reaching the threshold of about 0.3% of the elastic peak in specular geometry when further improvement was no longer possible. The detected trace amounts of oxygen, estimated to be around 2% of a monolayer, did not increase significantly after hours of measurements (see section C of supplementary information for details).

All experiments were performed at room temperature. Figure 1 shows typical angle-resolved EEL spectra taken along the $\bar{\Gamma}$ - \bar{M} direction (Figure 2b) for positive values of the momentum transfer parallel to the surface, q_{\parallel} (Figure 2c). A broad peak is observed to disperse as a function of q_{\parallel} with another non-dispersing loss peak due to traces of oxygen contaminants. The energy loss of the dispersing peak was determined via a multi peak fitting procedure. The corresponding q_{\parallel} was then calculated from energy and momentum conservation (see section B of supplementary information for a complete description of the method). The so determined experimental dispersion of the energy loss peak, which was measured up to 2 eV, is shown in Figure 2a, and is well below the conventional Be surface plasmon energy of about 13 eV^{15,16}. It is clearly not affected by changes in the scattering geometry and/or in incident energy of the electron beam. In the long-wavelength

limit, the energy of the new mode is found to approach zero linearly for vanishing values of the momentum component parallel to the surface. Our data clearly show the acoustic character of this excitation within the limits of the experimental errors. In our experiment we have probed the surface at low q_{\parallel} values of the first surface Brillouin zone (Figure 2, a and b). Due to the isotropic surface state dispersion around $\bar{\Gamma}$ (Figure 2d), the orientation of the electron scattering plane is not expected to have any influence on the dispersion of the new excitation, as confirmed by *ab initio* calculations for the $\bar{\Gamma}$ - \bar{K} direction. We have tried to probe the new acoustic excitation for positive and negative q_{\parallel} . All the data shown are for positive momentum transfer. In the negative momentum transfer spectra we have seen no well defined energy loss and that is presumably related to the narrow dipole lobe resulting in a low excitation probability¹⁷.

Metal surfaces such as Be(0001) and the (111) surfaces of noble metals support a partially occupied band of Shockley surface states with energies near the Fermi level. Their wave functions are strongly localized near the surface and decay exponentially into the solid thus forming a quasi 2D electron gas overlapping the 3D bulk electrons. While employing a local dielectric function to describe the 3D continuum⁷ has suggested that a complete screening of a 2D charge density *overlapping* a 3D plasma will prevent *any* low energy collective excitations to exist, we show that these experimental data can be interpreted as a novel type of collective electronic excitation (acoustic surface plasmon) of the quasi 2D surface charge distribution if a full non-local dynamical screening at the surface due to underlying 3D bulk electrons is considered. This collective mode corresponds to out-of-phase charge density oscillations of the 2D and 3D electron subsystems at a metal surface.

Information on collective electronic excitations at surfaces is obtained from the peak position of the imaginary part of the surface response function $g(\mathbf{q}_{\parallel}, \omega)$ which depends on the two-dimensional momentum transfer parallel to the surface \mathbf{q}_{\parallel} and the frequency ω ^{18,19} (we use atomic units, i.e. $e^2 = \hbar = m_e = 1$):

$$g(\mathbf{q}_{\parallel}, \omega) = \int d\mathbf{r} \int d\mathbf{r}' e^{q_{\parallel} z'} \chi(\mathbf{r}, \mathbf{r}', \omega) V_{ext}(\mathbf{r}', \omega), \quad (1)$$

where the external potential is of the form $V_{ext}(\mathbf{r}', \omega) = -\frac{2\pi}{q_{\parallel}} e^{q_{\parallel} z'} e^{i\mathbf{q}_{\parallel} \cdot \mathbf{r}'} e^{-i\omega t}$ and the non-local frequency-dependent density-response function of the interacting electron system $\chi(\mathbf{r}, \mathbf{r}', \omega)$ is calculated in the framework of time-dependent density-functional theory using the integral equation (in symbolic form) $\chi = \chi^0 + \chi^0(v + f_{xc})\chi$, where v is the bare Coulomb potential, χ^0 represents the density-response function of non-interacting electrons, and f_{xc} is the so-called exchange-correlation kernel chosen here to be zero (random-phase approximation). We calculate first the single particle energies and wave functions which describe the surface band structure. With these wave functions and energies we then compute χ^0 and then solve the integral equation for χ (see supplementary information section A).

The black dashed line shown in Figure 2a is the acoustic dispersion curve that has been predicted assuming a free-electron like behavior for the surface state on Be(0001) located in a wide 3D-energy gap around $\bar{\Gamma}^{16}$. The calculation agrees qualitatively with the experiment in the sense that both have an acoustic character, but the quantitative agreement is rather poor. The reason for this turns out to be the insufficient accuracy in describing the surface electron state dispersion. We are able to reproduce the experimental dispersion quantitatively by employing an *ab initio* description of the surface electronic structure and the surface response function. The

proper surface state dispersion around $\bar{\Gamma}$ (Figure 2d) deviates from the free-electron scenario. In the occupied part it is nearly parabolic with a binding energy of 2.7 eV at $\bar{\Gamma}$, in close agreement with photoemission measurements and previous calculations²⁰⁻²². Nevertheless, important differences between the actual surface-state band and a band of free electrons are (i) the considerable deviation from parabolic behavior above the Fermi level and (ii) the abrupt cut at the borders of the energy gap around 1 eV above the Fermi level. Using the *ab initio* surface state dispersion as a starting point for a calculation of the acoustic surface plasmon dispersion results in the red line in Figure 2a. Clearly, the agreement with the experimental data is much better, greatly increasing our confidence in the interpretation.

The acoustic surface plasmon results from the interplay of the partially occupied electronic surface state, acting as a 2D electron density overlapping in the same region of space with the bulk electron gas, and the long-range Coulomb interaction manifested in the form of 3D dynamical screening of the 2D surface electron density. It corresponds to the out-of-phase charge oscillations between 2D and 3D subsystems and its dispersion is mainly determined by the surface-state Fermi velocity v_F^{2D} and follows closely the upper edge of the continuum for electron-hole pair excitations within the surface-state band (Figure 2a). The situation on Be(0001), which has a high v_F^{2D} , is favorable for an experimental observation because in this case the new collective excitation is well defined up to relatively high energies of more than 1 eV. On other surfaces with a partially occupied surface-state band, such as the noble-metal (111) surfaces, the new mode is expected to be best defined at lower energies up to about several hundreds meV²³ thus making its EELS detection more difficult²⁴ – one needs to be careful when choosing the scattering geometry and

incident energy such that the scanned energy loss will cross the acoustic dispersion curve at low enough loss energies where electron-hole transitions from occupied 3D bulk states to unoccupied 2D surface states cannot occur. For its importance in electron and hole dynamics, however, this restriction is of little relevance since the low-energy region is of highest importance.

Acoustic surface plasmons, as reported here, owe their existence to the non-local screening due to bulk electrons at surfaces characterized by a partially occupied surface-state band lying in a wide bulk energy gap (Figure 2d) and as such they should be a common phenomenon on many metal surfaces. Moreover, since the acoustic plasmon dispersion follows closely the upper edge of electron-hole excitation, it will affect the electron dynamics near the Fermi level much more dramatically than regular 2D plasmons², which due to their $q_{\parallel}^{1/2}$ dispersion overlap in a much narrower range in energy-momentum space with the electron-hole continuum. The possibility to excite a collective mode at very low energies can therefore lead to new situations at metal surfaces due to the competition between the incoherent electron-hole excitations and the new collective coherent mode. Many phenomena, such as electron, phonon and adsorbate dynamics as well as chemical reactions with characteristic energies lower than few eV can be significantly influenced by the opening of a new low-energy decay channel such as the acoustic surface plasmon.

Of particular interest is the interaction of the acoustic surface plasmon with light. Since the slope of the acoustic surface plasmon dispersion, determined by v_F^{2D} , is about three orders of magnitude lower than the speed of light, the direct excitation of the new collective mode by light is not possible. However, the presence of nanometer-size objects at surfaces, such as atomic steps

or molecular structures can serve as a source of coupling between acoustic surface plasmons and light. The acoustic dispersion allows, at the same photon energy, for a collective surface excitation with a much lower associated wavelength than a regular 2D plasmon with its $q_{\parallel}^{1/2}$ dispersion. In this way, the new mode can serve as a tool to confine light in a broad frequency range up to optical frequencies on surface areas of a few nanometers thus ensuring the control of events at metal surfaces with both high spatial (nm) and temporal (fs) resolution. Another consequence of the acoustic character of the dispersion is that both phase and group velocity of the collective excitation are the same so that signals can be transmitted undistorted along the surface. Corroborated with the fact that a theoretically estimated decay length of the ASP of 100 nm to 1000 nm is expected for the medium (100 meV) to the far (10 meV) infrared, this is an appealing aspect for the field of nano-optics.

1. S. J. Allen and, D. C. T. & Logan, R. A. Observation of the Two-Dimensional Plasmon in Silicon Inversion Layers. *Phys. Rev. Lett.* **38**, 980–983 (1977).
2. Nagao, T., Hildebrandt, T., Henzler, M. & Hasegawa, S. Dispersion and Damping of a Two-Dimensional Plasmon in a Metallic Surface-State Band. *Phys. Rev. Lett.* **86**, 5747–5750 (2001).
3. March, N. H. & Tosi, M. P. Collective effects in condensed conducting phase including low-dimensional systems. *Adv. Phys.* **44**, 299–386 (1995).
4. Stern, F. Polarizability of a Two-Dimensional Electron Gas. *Phys. Rev. Lett.* **18**, 546–548 (1967).

5. Chaplik, A. V. Possible Crystallization of Charge Carriers in Low-Density Inversion Layers. *Sov. Phys. JETP* **35**, 395–398 (1972).
6. Ruvalds, J. Are plasmons the key to superconducting oxides? *Nature* **328**, 299 (1987).
7. Sarma, S. D. & Madhukar, A. Collective modes of spatially separated, two-component, two-dimensional plasma in solids. *Phys. Rev. B* **23**, 805–815 (1981).
8. Ritchie, R. H. Plasma Losses by Fast Electrons in Thin Films. *Phys. Rev.* **106**, 874–881 (1957).
9. Schuster, S. C., Swanson, R. V., Alex, L. A., Bourret, R. B. & Simon, M. I. Assembly and function of a quaternary signal transduction complex monitored by surface plasmon resonance. *Nature* **365**, 343–347 (1993).
10. Flatgen, G. *et al.* Two-Dimensional Imaging of Potential Waves in Electrochemical Systems by Surface Plasmon Microscopy. *Science* **269**, 668–671 (1995).
11. Barnes, W. L., Dereux, A. & Ebbesen, T. W. Surface plasmon subwavelength optics. *Nature* **424**, 824–830 (2003).
12. Lezec, H. *et al.* Beaming Light from a Subwavelength Aperture. *Science* **297**, 820–822 (2002).
13. Pendry, J. Playing Tricks with Light. *Science* **285**, 1687–1688 (1999).
14. Rocca, M., Valbusa, U., Gussoni, A., Maloberti, G. & Racca, L. Apparatus for adsorption studies. *Rev. Sci. Instrum.* **62**, 2172–2176 (1991).

15. Höchst, H., Steiner, P. & Hüfner, S. The conduction electron hole coupling in beryllium metal. *Phys. Lett.* **60A**, 69–71 (1977).
16. Silkin, V. M. *et al.* Novel low-energy collective excitation at metal surfaces. *Europhys. Lett.* **66**, 260–264 (2004).
17. Rocca, M. Low-energy EELS investigation of surface electronic excitations on metals. *Surf. Sci. Rep.* **22**, 1–71 (1995).
18. Persson, B. N. J. & Zaremba, E. Electron-hole pair production at metal surfaces. *Phys. Rev. B* **31**, 1863–1872 (1985).
19. Liebsch, A. *Electronic Excitations at Metal Surfaces* (Plenum Press, London, 1997).
20. Karlsson, U. O., Flodström, S. A., Engelhardt, R., Gädeke, W. & Koch, E. E. Intrinsic surface state on Be(0001). *Solid State Commun.* **49**, 711–714 (1984).
21. Bartynski, R. A., Jensen, E., Gustafsson, T. & Plummer, E. W. Angle-resolved photoemission investigation of the electronic structure of Be: Surface states. *Phys. Rev. B* **32**, 1921–1926 (1985).
22. Chulkov, E. V., Silkin, V. M. & Shirykalov, E. N. Surface electronic structure of Be(0001) and Mg(0001). *Surf. Sci.* **188**, 287–300 (1987).
23. Silkin, V. M., Pitarke, J. M., Chulkov, E. V. & Echenique, P. M. Acoustic surface plasmons in the noble metals Cu, Ag, and Au. *Phys. Rev. B* **72**, 115435–115441 (2005).

24. Politano, A., Chiarello, G., Formoso, V., Agostino, R. & Colavita, E. Plasmon of Shockley surface states in Cu(111): A high-resolution electron energy loss spectroscopy study. *Phys. Rev. B* **74**, 081401(R)–081404(R) (2006).

Supplementary information is linked to the online version of the paper at www.nature.com/nature and contains the following sections and figures: A. *Ab initio* calculation details, B. Extraction of the experimental dispersion, C. Oxygen influence on the Acoustic Surface Plasmon, Figures 1, 2, and 3.

Acknowledgements This work was supported in part by the National Science Foundation (B. D. and K. P.), and by the Istituto dei Materiali per l’Elettronica ed il Magnetismo of the Istituto Nazionale delle Ricerche (L. V, L. S. and M. R.), and by the Basque Departamento de Educacin, Universidades e Investigacin and the University of the Basque Country UPV/EHU; by the Spanish MEC (V. S, J. P, E. C, P. E, and D. F.); the Danish Natural Science Research Council (Ph. H.); and by the Programa Ramon y Cajal and Comunidad de Madrid (D. F).

Competing Interests The authors declare that they have no competing financial interests.

Correspondence and requests for materials should be addressed to K.P. (e-mail: karsten.pohl@unh.edu).

Figure 1 Families of Angle-Resolved EEL spectra taken at room temperature in the $\bar{\Gamma}$ - \bar{M} direction for two electron incident energies E_i and emergent scattering angles θ_s . The instrument employed a fixed analyzer angle θ_s with a variable incident electron beam angle θ_i ¹⁴. Each spectrum corresponds to a different electron momentum transfer component parallel to the surface q_{\parallel} . The spectra have been evenly spaced vertically for clarity. The additional, non dispersing, low frequency loss is due to the residual oxygen contamination.

Figure 2 Acoustic surface plasmon energy dispersion. (a) Experimental dispersion measured at room temperature and various incident electron energies and scattering angles; energy error bars are due to uncertainties in the multi peak deconvolution procedure of the EEL spectra while q_{\parallel} error bars represent the momentum integration window due to the finite angular acceptance of the EEL spectrometer (as described in supplementary information). Theoretical dispersion: the black dashed line shows the predicted acoustic surface plasmon dispersion obtained for a free-electron like surface state, the solid red line was calculated by using an *ab initio* Be(0001) surface band structure; (b) first surface Brillouin zone of Be(0001); (c) Scattering geometry in EEL spectra measurements. (d) *ab-initio* Be(0001) surface electronic band structure.

$E_i = 7.26\text{eV}; \theta_s = 63.3^\circ$

— $E_{\text{loss}} = 0.30\text{eV}; q_{\parallel} = 0.06 \text{ \AA}^{-1}$

— $E_{\text{loss}} = 0.40\text{eV}; q_{\parallel} = 0.08 \text{ \AA}^{-1}$

— $E_{\text{loss}} = 0.59\text{eV}; q_{\parallel} = 0.11 \text{ \AA}^{-1}$

— $E_{\text{loss}} = 0.73\text{eV}; q_{\parallel} = 0.12 \text{ \AA}^{-1}$

— $E_{\text{loss}} = 0.76\text{eV}; q_{\parallel} = 0.14 \text{ \AA}^{-1}$

— $E_{\text{loss}} = 0.80\text{eV}; q_{\parallel} = 0.16 \text{ \AA}^{-1}$

— $E_{\text{loss}} = 0.97\text{eV}; q_{\parallel} = 0.19 \text{ \AA}^{-1}$

— $E_{\text{loss}} = 1.42\text{eV}; q_{\parallel} = 0.25 \text{ \AA}^{-1}$

— $E_{\text{loss}} = 1.59\text{eV}; q_{\parallel} = 0.28 \text{ \AA}^{-1}$

Intensity [arb. units]

0 1000 2000 3000

Energy [meV]

$E_i = 10.74\text{eV}; \theta_s = 59.2^\circ$

— $E_{\text{loss}} = 0.70\text{eV}; q_{\parallel} = 0.12 \text{ \AA}^{-1}$

— $E_{\text{loss}} = 0.90\text{eV}; q_{\parallel} = 0.18 \text{ \AA}^{-1}$

— $E_{\text{loss}} = 1.30\text{eV}; q_{\parallel} = 0.23 \text{ \AA}^{-1}$

— $E_{\text{loss}} = 1.46\text{eV}; q_{\parallel} = 0.25 \text{ \AA}^{-1}$

— $E_{\text{loss}} = 1.60\text{eV}; q_{\parallel} = 0.29 \text{ \AA}^{-1}$

— $E_{\text{loss}} = 1.83\text{eV}; q_{\parallel} = 0.33 \text{ \AA}^{-1}$

— $E_{\text{loss}} = 1.87\text{eV}; q_{\parallel} = 0.35 \text{ \AA}^{-1}$

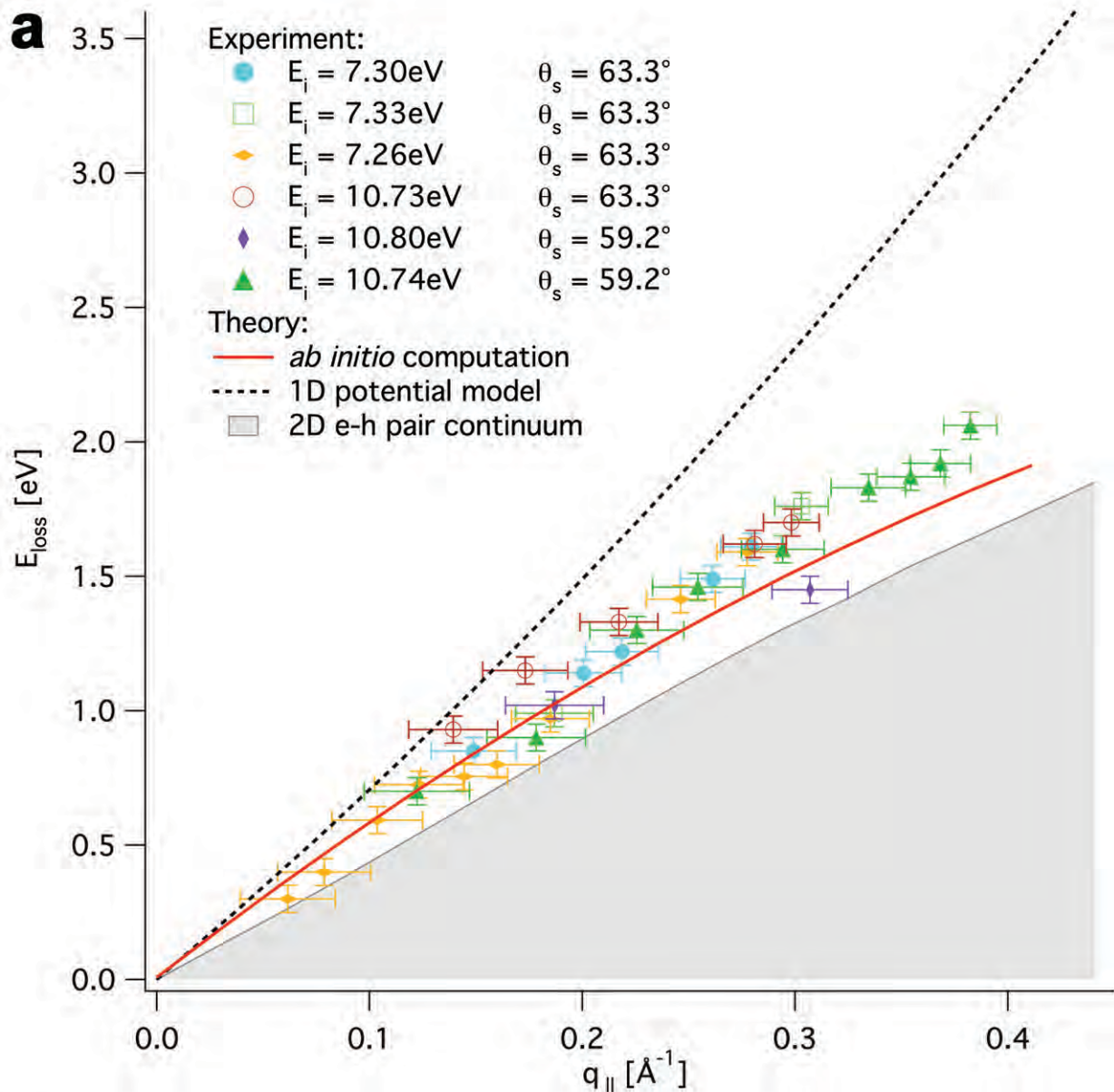
— $E_{\text{loss}} = 1.92\text{eV}; q_{\parallel} = 0.37 \text{ \AA}^{-1}$

— $E_{\text{loss}} = 2.06\text{eV}; q_{\parallel} = 0.38 \text{ \AA}^{-1}$

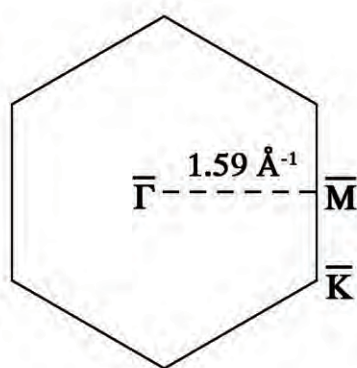
Intensity [arb. units]

0 1000 2000 3000

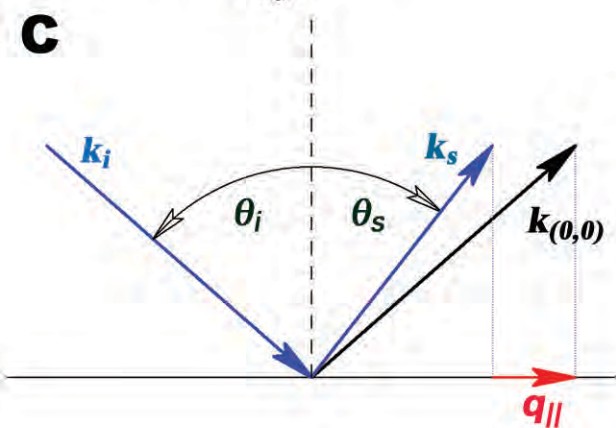
Energy [meV]



b



c



d

